Upwelling around Cabo Frio, Brazil: The importance of wind stress curl

Renato M. Castelao[1,2] and John A. Barth[1,2]

Received 9 November 2005; revised 16 December 2005; accepted 22 December 2005; published 2 February 2006.

[1] Data from the SeaWinds scatterometer on the QuikSCAT satellite are used to estimate upwelling around Cabo Frio, Brazil, due to Ekman transport and Ekman pumping. The region close to shore (up to 200 km from the coast) is characterized by negative wind stress curl (upwelling favorable) year-round, with maximum values during summer, and minimum values during fall. Integrated values from São Sebastião Island to Vitória reveal that during summer, Ekman pumping and Ekman transport are of the same magnitude in the region. Estimates of Ekman transport are relatively uniform along the coast during summer. Ekman pumping, on the other hand, is strongly enhanced between São Sebastião Island and Vitória, the region where the coldest water on satellite images is frequently found. This suggests that wind stress curl-driven upwelling is a major contributor to the coldest surface water being found near Cabo Frio. **Citation:** Castelao, R. M., and J. A. Barth (2006), Upwelling around Cabo Frio, Brazil: The importance of wind stress curl, *Geophys. Res. Lett.*, *33*, L03602, doi:10.1029/2005GL025182.

1. Introduction

[2] The Brazilian Southeast continental shelf, in the vicinity of Cabo Frio, is characterized by a strong cross-shelf sea surface temperature (SST) gradient, reflecting the influence of persistent upwelling of relatively cold waters [*Castro and Miranda*, 1998], especially during the austral spring and summer (Figure 1). During this period, the large-scale South Atlantic high-pressure center makes the prevailing winds blow from the northeast, with a large component parallel to the coast [*Rodrigues and Lorenzzetti*, 2001] as required for the development of coastal upwelling. During winter, on the other hand, winds blowing from the southwest (downwelling favorable) are frequent and intense (although not predominant) due to an increase in the frequency of frontal passages.

[3] Previous studies have shown a high correlation between surface cold water events and easterly-northeasterly winds in the region [*Allard*, 1955; *Emílsson*, 1961; *Ikeda et al.*, 1974], and suggest that coastal upwelling produces the penetration of cold water onto the shelf. Uniform alongshore winds push water offshore in a surface Ekman layer due to the Earth's rotation. To compensate for the loss of mass near the coast, nutrient-rich, deeper water is brought toward the sea surface. We will refer to this upwelling process as "Ekman transport". The nutrient enrichment of the water column plays a key factor supporting the region's fisheries production [*Matsuura*, 1996].

[4] Recent studies have shown other mechanism can play a significant role in the pumping of cold waters onto the shelf in the region and in producing spatial variability in upwelling. *Campos et al.* [2000] and *Castelao et al.* [2004] have used observations and numerical modeling to shown the importance of shelf-break upwelling induced by cyclonic meanders of the Brazil Current. In a series of process-oriented numerical simulations, *Rodrigues and Lorenzzetti* [2001] showed that coastline irregularities and bottom topography effects also affect the spatial pattern of upwelling in the region.

[5] Insufficient meteorological data has so far prevented evaluation of the importance of the wind stress curl in the upwelling around Cabo Frio. In that process (Ekman pumping), wind stress curl generates ocean-surface divergence (convergence), forcing upward (downward) water movements. Analyses in other ocean regions (e.g., the California Current System) have shown that Ekman pumping from wind stress curl can be as important as Ekman transport from alongshore winds [*Pickett and Paduan*, 2003]. The availability of satellite wind data from the polar-orbiting QuikSCAT satellite allows for the Ekman pumping effect to be quantified off southeast Brazil for the first time. The QuikSCAT data have already been successfully used for estimating Ekman transport and Ekman pumping in other upwelling regions [*Huyer et al.*, 2005].

2. Data and Methods

[6] A description of the SeaWinds scatterometer on the QuikSCAT satellite is given by *Freilich et al.* [1994]. The SeaWinds scatterometer is a scanning microwave radar that infers the surface wind stress from measurements of radar backscatter from the roughness of the sea surface at multiple antenna look angles [*Naderi et al.*, 1991]. Scatterometer wind retrievals are accurate to better than 2 m s^{-1} in speed and 20° in direction, which is essentially equivalent to the accuracy of in situ point measurements from buoys [*Freilich and Dunbar*, 1999]. The QuikSCAT spatial resolution is about 25 km.

[7] In this study, wind data spanning a 5-year long period (2000–2004) are used. In order to obtain wind-driven upwelling estimates, we follow *Pickett and Paduan* [2003]. The Ekman transport at every coastal grid point, M (m^3 s^{-1} per meter of coast), was calculated from [*Smith*, 1968]

$$M = \frac{\vec{\tau} \cdot \hat{t}}{\rho f} \quad (1)$$

[1]College of Oceanic and Atmospheric Sciences, Oregon State University, Corvallis, Oregon, USA.
[2]Cooperative Institute for Oceanographic Satellite Studies, Oregon State University, Corvallis, Oregon, USA.

0094-8276/06/2005GL025182$05.00

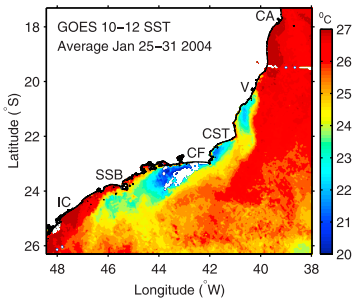

Figure 1. SST from the GOES 10–12 satellite averaged over 7 days (25–31) during January (austral summer), 2004, showing coastal upwelling near Cabo Frio. Clouds are marked in white. IC, Ilha Comprida; SSB, São Sebastião Island; CF, Cabo Frio; CST, Cabo de São Tomé; V, Vitória; CA, Caravelas.

where $\vec{\tau}$ is the wind stress vector, $\hat{t}$ is a unit vector tangent to the local coastline (obtained by fitting a straight line through a 50-km section of a coastline centered at the coastal point), ρ is the density of seawater (1024 kg m^{-3}) and f is the Coriolis parameter.

[8] The Ekman pumping velocity, w (m s^{-1}), was calculated from [*Smith*, 1968]

$$w = \hat{k} \cdot \nabla \times \frac{\vec{\tau}}{\rho f} \tag{2}$$

where $\hat{k}$ is a unit vector in the local vertical direction. The wind stress curl field was derived by first-order differencing the wind stress field. The Ekman pumping velocities were then integrated out to 200-km offshore (approximately the distance offshore where the negative wind stress curl extends) in order to obtain a vertical transport at every coastal grid point (m^3 s^{-1} per meter of coast) that could be compared with the Ekman transport obtained by (1).

[9] By integrating both the Ekman transport and the Ekman pumping estimates along the coast, an estimation of the net upwelling in the region was obtained.

[10] Unfortunately, there is a gap in the scatterometer measurements within about 30 km of the coast because of land contamination in the radar antenna sidelobes. Since the predominant winds in the study region around Cabo Frio are from the northeast, and the wind stress curl is generally negative, the 30-km region experiences weaker winds on average. This is supported by wind measurements obtained by a research cruise during 1971 [*Ikeda et al.*, 1974]. When this is true, equations (1) and (2) will provide an overestimation of the Ekman transport, and an underestimation of the Ekman pumping.

3. Seasonal Variability of the Wind Stress and Wind Stress Curl Fields

[11] The summer- and winter-averaged wind stress is shown on Figure 2. The wind stress maximum during summer occurs just southeast of Cabo Frio. To the north of Cabo de São Tomé, winds are slightly directed onshore. Although there is considerable spatial variability in the offshore region, winds close to the coast between Vitória and Cabo de São Tomé are less spatially variable, with weaker magnitudes compared to offshore. To the southwest of Cabo Frio, winds are weaker, but are more closely aligned with the coastline orientation. During winter, northeasterly winds decrease in magnitude in the whole region, and are more directed onshore in the north, consistent with observations that upwelling is diminished during this period.

[12] The wind stress curl field also has strong seasonal variability (Figure 3), although negative values are found year-round in a band extending 150–250 km from the coast. Offshore values are generally positive and small. Maximum negative curl (upwelling favorable) close to the coast occurs during summer, extending all the way from just north of Vitória to São Sebastião Island (SSB). Note that this is approximately the same region with the coldest water apparent in Figure 1.

[13] The wind stress curl strongly diminishes during fall, being at its annual minimum. Winter is characterized by increased curl to the southwest of Cabo Frio, but with little intensification to the north. Intensification of wind stress curl in the north occurs during spring. The extent of the region occupied by negative wind stress curl during spring is roughly the same size as during summer, although with weaker magnitudes. The regions to the north of Vitória or to the south of SSB are characterized by weak wind stress curl during all seasons.

4. Ekman Transport and Ekman Pumping

[14] In order to quantify the relative importance of upwelling driven by coastal divergence (Ekman transport)

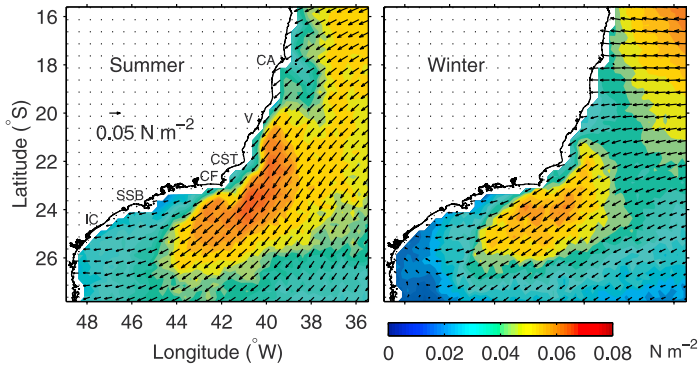

Figure 2. QuikSCAT summer and winter (2000–2004) vector average wind stress and vector magnitudes (N m^{-2}). Every second vector is shown. See Figure 1 for acronyms.

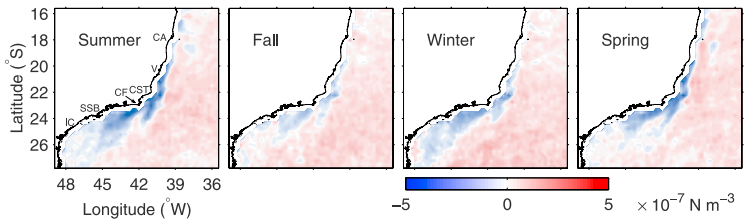

Figure 3. QuikSCAT mean seasonal (2000–2004) wind stress curl (10^{-7} N m^{-3}). See Figure 1 for acronyms.

and wind stress curl-driven upwelling, estimates of Ekman transport and Ekman pumping were integrated along the coast from Vitória to SSB (Figure 4). Total upwelling estimates were obtained by summing Ekman transport and Ekman pumping.

[15] Both transport estimates have significant seasonal variability. During summer, both Ekman transport and Ekman pumping are high, and of similar magnitudes. Ekman pumping is on average 20% weaker than Ekman transport, almost doubling the amount of upwelling one would predict by just considering upwelling due to coastal divergence. During summer, 45% of the total wind driven upwelling is actually due to Ekman pumping (peak in January). Curl-driven upwelling strongly decreases after March, as could be expected from Figure 3. Values remain small throughout fall, but increase again later in the year. Ekman transport magnitudes are also at a minimum during May, increasing after that. During spring, the local intensification in the wind stress magnitude (located offshore during summer; see Figure 2) moves inshore to just south of Vitória (not shown), substantially increasing the Ekman transport. During this period, coastal divergence is responsible for roughly 70% of the total upwelling.

5. Why is Upwelling Enhanced Around Cabo Frio?

[16] In order to assess the spatial variability in the contributions from both mechanisms to the total upwelling, Ekman transport and transport due to Ekman pumping are plotted for each season as a function of alongshore distance, from Caravelas to Ilha Comprida (Figure 5). Values were smoothed using a 100 km wide running mean. The SST data plotted in Figure 5 is only shown as an example, since it is from a single week during summer 2004, and not a 5 year average.

[17] During summer, upwelling due to Ekman transport varies little alongshore, with an approximate 25% decrease in the magnitude to the south of Cabo Frio. Note that the Ekman transport magnitudes to the north of Vitória and to the south of SSB are close to the upwelling magnitude between these limits. Ekman pumping, on the other hand, is small outside these limits, but is comparable to Ekman

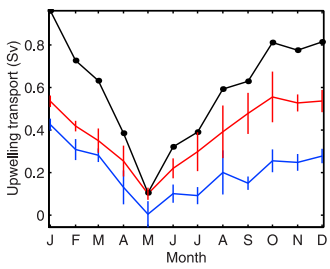

Figure 4. Monthly upwelling estimates (5 year average, 2000–2004) integrated from Vitória to São Sebastião Island. Total upwelling (black) is the sum of Ekman transport (red) and Ekman pumping (blue). Vertical lines are ±1 standard error of the mean.

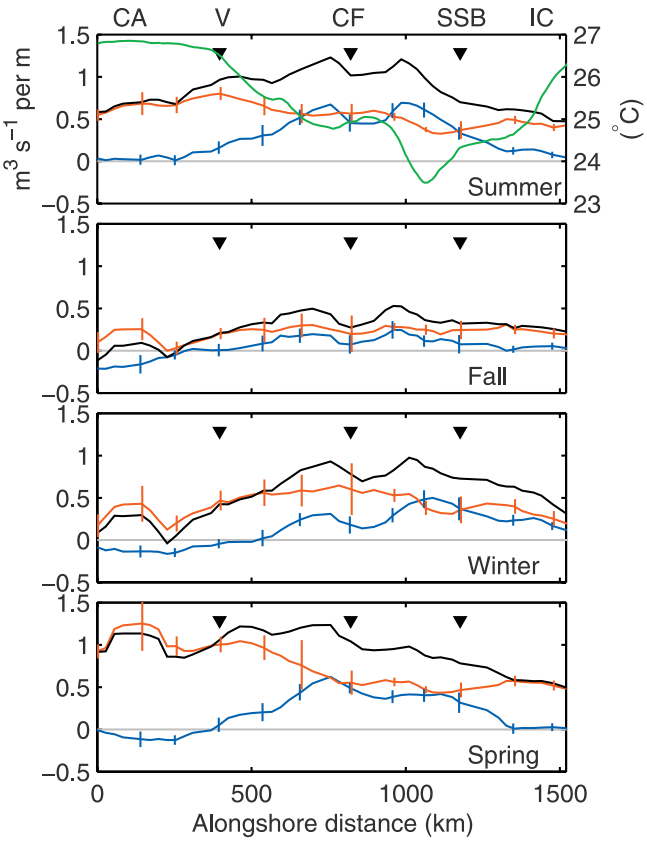

Figure 5. Seasonal alongshore estimates of wind-driven upwelling (5 year average, 2000–2004), from Caravelas (CA) to Ilha Comprida (IC). Upside-down triangles show location of Vitória (V), Cabo Frio (CF), and São Sebastião Island (SSB), the approximated limits for the region of enhanced upwelling (see Figure 1). Total upwelling (black) is the sum of Ekman transport (red) and Ekman pumping (blue). Vertical lines are ±1 standard error of the mean. The green line in the top panel is the averaged temperature within 200 km from the coast from the one week composite shown in Figure 1.

transport on the region where the coldest water is found, effectively doubling the total upwelling in this region compared to regions to the north or to the south. Just north of SSB and Cabo Frio, Ekman pumping is actually more important in causing localized upwelling than Ekman transport. Therefore, Ekman pumping combined with increased upwelling controlled by topographic effects [*Rodrigues and Lorenzzetti*, 2001] could help explain the occurrence of the coldest waters near Cabo Frio during summer.

[18] Although small during fall, curl-driven upwelling is again important around and to the south of Cabo Frio during winter and spring, doubling the total amount of upwelling. The dominance of coastal upwelling during spring seen in Figure 4 actually occurs to the north of Cabo Frio (as the local maximum in the wind intensity moves close to the coast), with both mechanism having equal importance between Cabo Frio and SSB.

6. Discussion and Conclusions

[19] It is a well-known fact that upwelling is enhanced in the vicinity of Cabo Frio, Brazil, and that it has a significant effect on fisheries in the region. The majority of previous studies attributed the upwelling in the region to coastal divergence (due to Ekman transport close to the coast). Recently, studies suggested that topographic effects and meander induced shelf break upwelling could also be important. The lack of high-resolution wind data with good temporal and spatial coverage prevented the assessment of the importance of upwelling driven by Ekman pumping (due to wind stress curl). High-spatial resolution wind data from the QuikSCAT satellite makes quantifying that process possible for the first time.

[20] The region between Vitória and SSB is characterized by negative wind stress curl year-round, with maximum values during summer and minimum during fall. Estimates during summer reveal that Ekman pumping is strongly enhanced between these limits, the same region where the coldest water is frequently observed. Ekman transport estimates are less variable alongshore. It is hypothesized that the localized increase in Ekman pumping added to the Ekman transport contributes significantly to the frequent observation of cold waters found near Cabo Frio. It is important to realize that the QuikSCAT data does not extend within 30 km from the coast. Therefore, the present analysis does not include smaller, headland-scale features that could lead to wind stress curl.

[21] The wind stress vector is on average along the SST front, leading to the interesting possibility of a positive feedback between the SST field and the wind curl. As summarized by *Chelton et al.* [2004], surface wind speeds are lower over cool water and higher over warm water, via the influence of air-sea heat flux on the marine atmospheric boundary layer. Lateral variations where winds blow parallel to isotherms (as near Cabo Frio) generate curl. The magnitudes of the curl perturbations are proportional to the magnitudes of the crosswind SST gradients. Therefore, the negative wind stress curl in the region causes upwelling and decrease of the SST, which in turn could increase the magnitude of the negative wind stress curl.

[22] Finally, results suggest that numerical modeling efforts to simulate the circulation in the region and to understand its dynamics should include spatially variable wind forcing, to accurately represent the wind stress curl field.

[23] **Acknowledgments.** This paper was prepared under award NA03NES4400001 from the National Oceanic and Atmospheric Administration, NOAA U.S. Department of Commerce. The statements, findings, conclusions, and recommendations are those of the authors and do not necessarily reflect the views of the NOAA or the U.S. Department of Commerce. Additional funding was provided by the Brazilian Research Council (CNPq grant 200147/01-3, RC) and by the National Science Foundation (grants OCE-9907854 and OCE-0001035, JB).

References

Allard, P. (1955), Anomalies dans le temperature de l'eau de la mer observees au Cabo Frio au Bresil, *Bull. Inf. Com. Oceanogr. Etude Cotes*, *7*(2), 58–63.

Campos, E. J. D., D. Velhote, and I. C. A. da Silveira (2000), Shelf break upwelling driven by Brazil Current cyclonic meanders, *Geophys. Res. Lett.*, *27*, 751–754.

Castelao, R. M., E. J. D. Campos, and J. L. Miller (2004), A modelling study of coastal upwelling driven by wind and meanders of the Brazil Current, *J. Coastal Res.*, *20*(3), 662–671.

Castro, B. M., and L. B. Miranda (1998), Physical oceanography of the western Atlantic continental shelf located between 4°N and 34°S, in *The Sea*, vol. 11, edited by A. R. Robinson and K. H. Brink, pp. 209–251, John Wiley, Hoboken, N. J.

Chelton, D. B., M. G. Schlax, M. H. Freilich, and R. F. Milliff (2004), Satellite measurements reveal persistent small-scale features in ocean winds, *Science*, *303*, 978–983.

Emílsson, I. (1961), The shelf and coastal waters off southern Brazil, *Bol. Inst. Oceanogr.*, *11*(2), 101–112.

Freilich, M. H., and R. S. Dunbar (1999), The accuracy of the NSCAT 1 vector winds: Comparisons with National Data Buoy Center buoys, *J. Geophys. Res.*, *104*, 11,231–11,246.

Freilich, M. H., D. G. Long, and M. W. Spencer (1994), SeaWinds: A scanning scatterometer for ADEOS II—Science overview, paper presented at International Geoscience and Remote Sensing Symposium, Inst. of Electr. and Electron. Eng., Pasadena, Calif.

Huyer, A., J. H. Fleishbein, J. Keister, P. M. Kosro, N. Perlin, R. L. Smith, and P. A. Wheeler (2005), Two coastal upwelling domains in the northern California Current System, *J. Mar. Res.*, *63*, 901–929.

Ikeda, Y., L. B. Miranda, and I. C. Miniussi (1974), Observations on stages of upwelling in the region of Cabo Frio (Brazil) as conducted by continuous surface temperature and salinity measurements, *Bol. Inst. Oceanogr.*, *23*, 33–46.

Matsuura, Y. (1996), A probable cause of recruitment failure of Brazilian Sardine (*Sardinella aurita*) population during the 1974/75 spawning season, *S. Afr. J. Mar. Sci.*, *17*, 29–35.

Naderi, F. M., M. H. Freilich, and D. G. Long (1991), Spaceborne radar measurement of wind velocity over the ocean: An overview of the NSCAT scatterometer system, *Proc. IEEE*, *79*, 850–866.

Pickett, M. H., and J. D. Paduan (2003), Ekman transport and pumping in the California Current based on the U.S. Navy's high-resolution atmospheric model (COAMPS), *J. Geophys. Res.*, *108*(C10), 3327, doi:10.1029/2003JC001902.

Rodrigues, R. R., and J. A. Lorenzzetti (2001), A numerical study of the effects of bottom topography and coastline geometry on the Southeast Brazilian coastal upwelling, *Cont. Shelf Res.*, *21*, 371–394.

Smith, R. L. (1968), Upwelling, *Oceanogr. Mar. Biol. Annu. Rev.*, *6*, 11–46.

J. A. Barth and R. M. Castelao, College of Oceanic and Atmospheric Sciences, Oregon State University, Corvallis, OR 97331-5503, USA. (castelao@coas.oregonstate.edu)